The Earth's Core:

An Approach from First Principles

G. David Price[1], D. Alfè[1, 2], L. Vočadlo[1], and M.J. Gillan[2]

[1]Research School of Earth Sciences, Birkbeck and University College London, Gower Street, London WC1E 6BT, UK.

[2]Department of Physics and Astronomy, University College London, Gower Street, London WC1E 6BT, UK.

Abstract

The Earth's core is largely composed of iron (Fe), alloyed with less dense elements such as sulphur, silicon and/or oxygen. The phase relations and physical properties of both solid and liquid Fe-alloys are therefore of great geophysical importance. As a result, over the past fifty years the properties of Fe and its alloys have been extensively studied experimentally. However, achieving the extreme pressures (up to 360 GPa) and temperatures (~6000K) found in the core provide a major experimental challenge, and it is not surprising that there are still considerable discrepancies in the results obtained by using different experimental techniques. In the past fifteen years quantum mechanical techniques have been applied to predict the properties of Fe. Here we review the progress that has been made in the use of first principles methods in the study of Fe and its alloys, and focus upon the use of *ab initio* methods to model and interpret (i) the structure and properties of pure solid and liquid Fe under core conditions, (ii) the possible composition and thermal structure of the core, and (iii) the origin of inner core anisotropy.

Introduction

Knowing about the nature of the Earth's core lies at the heart of understanding the state of our planet. Today, we believe that the core is the source of the Earth's magnetic field, and that heat-flow from the core contributes significantly to driving mantle convection, and hence ultimately contributes to plate tectonics and the resulting evolution of the planet's surface. What we know of the details of the core's structure comes largely from seismology. Although previously inferred to exist from a knowledge of the mass and moment of inertia of the Earth, the presence of the Earth's core was only firmly established from seismology by Oldfield in 1906. Further seismological study enabled Guttenberg to determine the depth of the core-mantle boundary to be ~2890 km, and in 1936 Lehmann discovered that there existed an inner core (with a radius now known to be ~1220 km). It was not until 35 years later that Dziewonski and Gilbert (1971) definitely proved that the inner core was a solid region within the surrounding liquid outer core. Seismology has subsequently shown that the inner core is anisotropic, with seismic waves travelling faster parallel to the poles than in the equatorial plane (e.g. Creager, 1992), and most recently seismic measurements have been interpreted as showing that the Earth's solid inner core is even more structurally complex. The detailed interpretations of data differ, but all workers (e.g. Song and Helmberger, 1998; Ishii and Dziewonski, 2002; Beghein and Trampert, 2003) conclude that the inner core exhibits a significant degree of layering, which may either reflect the changing history of core crystallisation and deformation, or the occurrence of an unidentified change in the core-forming phase.

The fact that the core is largely composed of Fe was firmly established as a result of Birch's (1952) analysis of mass-density/sound-wave velocity systematics. Today we believe that the outer core is about 6 to10% less dense than pure liquid Fe, while the solid inner core is a few percent less dense than crystalline Fe (e.g. Poirier, 1994a). From cosmochemical and other considerations, it has been suggested (e.g. Poirier, 1994b; Allègre et al., 1995; McDonough and Sun, 1995) that the alloying elements in the core might include S, O, Si, H and C. It is also probable that the core contains minor amounts of other elements, such as Ni and K. The exact temperature profile of the core is still controversial (e.g. Alfè et al., 2002a), but it is generally held that the inner core is crystallising from the outer core as the Earth slowly cools, and that (as a result of the work outlined below) core temperatures are in the range ~4000-5500K, while the pressure at the centre of the Earth is ~360GPa.

Before a full understanding of the chemically complex core can reached, it is necessary to understand the properties and behaviour at high pressure (P) and temperatures (T) of its primary constituents, namely metallic Fe and its alloys. Experimental techniques have evolved rapidly in the past years, and today using diamond anvil cells or shock experiments the study of minerals at pressures up to ~200GPa and temperatures of a few thousand Kelvin is possible. These studies, however, are still far from routine, and results from different groups are often in conflict (see for example reviews by Poirier, 1994b; Shen and Heinz, 1998; Stixrude and Brown, 1998; Boehler, 2000). As a result, therefore, in order to complement these existing experimental studies and to extend the range of pressure and temperature over which we can model the Earth, computational mineral physics has, in the past decade, become an established and growing discipline.

Within computational mineral physics a variety of atomistic simulation methods (developed originally in the fields of solid state physics and theoretical chemistry) are used. These techniques can be divided approximately into those that use some form of interatomic potential model to describe the energy of the interaction of atoms in a mineral as a function of atomic separation and geometry, and those that involve the approximate solution of Schrödinger's equation to calculate the energy of the mineral species by quantum mechanical techniques. For the Earth sciences, the accurate description of the behaviour of minerals as a function of temperature is particularly important, and computational mineral physics usually uses either lattice dynamics or molecular dynamics methods to achieve this important step. The relatively recent application of all of these advanced condensed matter physics methods to geophysics has only been possible by the very rapid advances in the power and speed of computer processing. Techniques, which in the past were limited to the study of structurally simple compounds, with small unit cells, can today be applied to describe the behaviour of complex, low symmetry structures (which epitomise most minerals) and liquids.

In this paper, we will focus on recent studies of Fe and its alloys, which have been aimed at predicting their geophysical properties and behaviour under core conditions. We will contrast what is known from experiment or approximate theory, with the developing insight which is coming from computational mineral physics research. Although interatomic potentials have been used to study Fe (e.g. Matsui and Anderson, 1997), many of its properties are very dependent upon a precise description of its metallic nature and can only be modelled accurately by quantum mechanical methods. Thus, below we briefly introduce the essential *ab initio* techniques used in the most recent studies of Fe alloys (see also Stixrude et al., 1998; Vočadlo et al., 2003; Steinle-Neumann et al., 2003). We then present a discussion of the structure of the stable phase of Fe at

core pressures and temperatures, its melting behaviour at core pressures, *ab initio* estimates of the viscosity of the liquid core, estimates of the composition of the core and its predicted thermal structure. We conclude with a materials-based discussion of the interpretation of the seismic structure of the inner core, and conclude by high lighting some of the topics which must be studied in greater detail in the future.

Quantum Mechanical Simulations

Ab initio simulations are based on the description of the electrons within a system in terms of a quantum mechanical wave function, ψ, the energy and dynamics of which is governed by the general Schrödinger equation for a single electron:

$$i\hbar\frac{\partial\psi}{\partial t} = -\frac{\hbar^2}{2m}\nabla^2\psi + V(r)\psi \qquad (1)$$

where V(r) is the potential energy of the system and the other terms take their usual meaning. In minerals, however, it is necessary to take into account all of the electrons within the crystal, so the energy, E, of a many electron wave function, Ψ, is required:

$$E\Psi(r_1, r_2, ...r_N) = \left(\sum -\frac{\hbar^2}{2m}\nabla^2 + V_{ion} + V_{e\text{-}e}\right)\Psi(r_1, r_2, ...r_N) \qquad (2)$$

In a confined system, the electrons experience interactions between the nuclei and each other. This interaction may be expressed in terms of an ionic contribution and a Coulombic

contribution (the second and third terms within the brackets). Energy minimisation techniques may be applied in order to obtain the equilibrium structure for the system under consideration.

Unfortunately, the complexity of the wave function, Ψ, for an N electron system scales as M^N, where M is the number of degrees of freedom for a single electron wave function, ψ. This type of problem cannot readily be solved for large systems due to computational limitations, and therefore the exact solution to the problem for large systems is intractable. However, there are a number of approximations that may be made to simplify the calculation, whereby good predictions of the structural and electronic properties of materials can be obtained by solving self-consistently the one-electron Schrödinger equation for the system, and then summing these individual contributions over all the electrons in the system (for more detailed reviews see Gillan (1997) and Stixrude et al. (1998)). Fe and its alloys have been studied extensively by a number of groups (e.g., see Vočadlo et al., 2003; Steinle-Neumann et al., 2003), and it is now well established that *ab initio* calculations give an accurate description of all the key properties of Fe. The calculations performed by us and others (e.g. Steinle-Neumann et al., 2003) are based on Density Functional Theory (DFT), generally within the Generalised Gradient Approximation (GGA). Our calculations have been performed using the VASP code (Kresse and Furthmüller, 1996), and most recently we have used the Projected-Augmented Wave (PAW) method (Blöchl, 1994) to calculate the total energy of the system. The PAW method is closely related to the ultra-soft pseudopotential method and has been shown to give results that agree accurately with all-electron methods (Alfè et al., 2000, 2001).

To study Fe under core conditions, however, we need not only to explore the energetics of bonding, but we are also concerned with the effect of temperature on the system. This requires us

to calculate the Gibbs free energy of the systems, which can be done either using lattice dynamic or molecular dynamic methods. Lattice dynamics is a semi-classical approach that uses the quasiharmonic approximation (QHA) to describe a cell in terms of independent quantised harmonic oscillators, the frequencies of which vary with cell volume, thus allowing for a description of thermal expansion (e.g. Born and Huang, 1954). The motions of the individual particles are treated collectively as lattice vibrations or phonons, and the phonon frequencies, $\omega(q)$, are obtained by solving:

$$m\omega^2(q)e_i(q) = D(q)e_j(q) \qquad (3)$$

where m is the mass of the atom, and the dynamical matrix, D(q), is defined by:

$$D(q) = \sum_{ij}\left(\frac{\partial^2 U}{\partial u_i \partial u_j}\right)\exp(iq.r_{ij}) \qquad (4)$$

where r_{ij} is the interatomic separation, and u_i and u_j are the atomic displacements from their equilibrium position. For a unit cell containing N atoms, there are 3N eigenvalue solutions ($\omega^2(q)$) for a given wave vector q. There are also 3N sets of eigenvectors ($e_x(q)$, $e_y(q)$, $e_z(q)$) which describe the pattern of atomic displacements for each normal mode.

The vibrational frequencies of a lattice can be calculated *ab initio*, by standard methods such as the small-displacement method (e.g. Kresse et al., 1995). Having calculated the vibrational frequencies, a number of thermodynamic properties may be calculated using standard statistical mechanical relations, which are direct functions of these vibrational frequencies. Thus for example the Helmholtz free energy is given by:

$$F = k_B T \sum_i^M \left(\frac{x_i}{2} + \ln(1 - e^{-x_i}) \right) \quad (5)$$

where $x_i = h\omega_i/k_B T$, and the sum is over all the M=3N normal modes. Modelling the effect of pressure is essential if one is to obtain accurate predictions of phenomena such as phase transformations and anisotropic compression. This problem is now routinely being solved using codes that allow constant stress, variable geometry cells in both static and dynamic simulations. In the case of lattice dynamics, the mechanical pressure is calculated from strain derivatives, whilst the thermal kinetic pressure is calculated from phonon frequencies (e.g. Parker and Price, 1989). The balance of these forces can be used to determine the variation of cell size as a function of pressure and temperature.

Molecular dynamics is routinely used for medium to high temperature simulations of minerals and in all simulations of liquids, where lattice dynamics is of course inapplicable. The method is essentially classical, and its details are presented in, for example, Allen and Tildesley (1987). The interactions between the atoms within the system have traditionally been described in terms of the interatomic potential models mentioned earlier, but instead of treating the atomic motions in terms of lattice vibrations, each ion is treated individually. As the system evolves, the required dynamic properties are calculated iteratively at the specified pressure and temperature. The ions are initially assigned positions and velocities within the simulation box; their co-ordinates are usually chosen to be at the crystallographically determined sites, whilst their velocities are equilibrated such that they concur with the required system temperature, and such that both energy and momentum is conserved. In order to calculate subsequent positions and velocities, the forces acting on any individual ion are then calculated from the first derivative of the potential function, and the new position and velocity of each ion may be calculated at each time-

step by solving Newton's equation of motion. Both the particle positions and the volume of the system, or simulation box, can be used as dynamical variables, as is described in detail in Parrinello and Rahman (1980). The kinetic energy, and therefore temperature, is obtained directly from the velocities of the individual particles. With this explicit particle motion, the anharmonicity is implicitly accounted for at high temperatures.

Because of advances in computer power, it is now possible to perform *ab initio* molecular dynamics (AIMD), with the forces calculated fully quantum mechanically instead of relying upon the use of interatomic potentials. The first pioneering work in AIMD was that of Car and Parrinello (1985), who proposed a unified scheme to calculate *ab initio* forces on the ions and keep the electrons close to the Born-Oppenheimer surface while the atoms move. We have used in the work summarized below an alternative approach, in which the dynamics are performed by explicitly minimizing the electronic free energy functional at each time step. This minimization is more expensive than a single Car-Parrinello step, but the cost of the step is compensated by the possibility of making longer time steps.

The Properties of Fe under Core Conditions

The High P Structure of Fe

Before we can even begin to provide a materials based interpretation of the composition and structure of the core, we must understand the behaviour of its primary constituent (Fe) under core conditions. At ambient conditions, Fe adopts a body centred cubic (*bcc*) structure, that transforms with temperature to a face centred cubic (*fcc*) form, and with pressure transforms to

a hexagonal close packed (*hcp*) phase, ε Fe. The high P/T phase diagram of pure iron itself however is still controversial (see Figure 1 and also the discussions in Stixrude and Brown (1998), Anderson (2003), and Steinle-Neumann et al., (2003)). Various diamond anvil cell (DAC) based studies have been interpreted as showing that *hcp* Fe transforms at high temperatures to a phase which has variously been described as having a double hexagonal close packed structure (*dhcp*) (Saxena et al., 1996) or an orthorhombicly distorted *hcp* structure (Andrault et al., 1997). Furthermore, high pressure shock experiments have also been interpreted as showing a high pressure solid-solid phase transformation (Brown and McQueen, 1986; Brown, 2001), which has been suggested could be due to the development of a *bcc* phase (Matsui and Anderson, 1997). Other experimentalists, however, have failed to detect such a post-*hcp* phase (e.g. Shen et al., 1998; Nguyen and Holmes, 1999), and have suggested that the previous observations were due either to minor impurities or to metastable, strain-induced behaviour.

Further progress in interpreting the nature and evolution of the core would be severely hindered if the uncertainty concerning the crystal structure of the core's major chemical component remained unresolved. Such uncertainties can be resolved, however, using *ab initio* calculations, which we have shown provide an accurate means of calculating the thermoelastic properties of materials at high P and T (e.g. Vočadlo et al., 1999). Thermodynamic calculations on *hcp* Fe and *fcc* Fe at high P/T were reported by Wasserman et al. (1996) and by Stixrude et al. (1997). They used *ab initio* calculations to parameterise a tight-binding model; the thermal properties of this model were then obtained using the particle-in-a-cell method (see also Steinle-Neumann et al., (2003) for a review). The calculations that we performed (Vočadlo et al., 1999) to determine the high P-T structure of Fe, were the first in which *fully ab initio*, non-parameterised methods

were used, in conjunction with quasiharmonic lattice dynamics, to obtain free energies under core conditions of all the proposed candidate Fe structures.

Spin polarized simulations were initially performed on candidate phases (including a variety of distorted *bcc* and *hcp* structures and the *dhcp* phase) at pressures ranging from 325 to 360 GPa. These revealed, in agreement with Söderlind et al. (1996), that under these conditions only *bcc* Fe has a residual magnetic moment and all other phases have zero magnetic moments. It should be noted however, that the magnetic moment of *bcc* Fe disappears when simulations are performed at core pressures and an electronic temperature of >1000K, indicating that even *bcc* Fe will have no magnetic stabilisation energy under core conditions. We found that at these pressures, both the *bcc* and the suggested orthorhombic polymorph of iron (Andrault et al., 1997) are mechanically unstable. The *bcc* phase can be continuously transformed to the *fcc* phase (confirming the findings of Stixrude and Cohen, 1995), while the orthorhombic phase spontaneously transforms to the *hcp* phase, when allowed to relax to a state of isotropic stress. In contrast, *hcp*, *dhcp* and *fcc* Fe remain mechanically stable at core pressures, and we were therefore able to calculate their phonon frequencies and free energies.

Although no experimentally determined phonon-dispersion curves exist for *hcp* Fe, the quality of our calculations can be gauged by comparing the calculated phonon dispersion for *bcc* Fe (done using fully spin polarised calculations) at ambient pressure, with the existing experimental data. Figure 2 shows the phonon dispersion curve for magnetic *bcc* Fe at ambient conditions compared with data obtained from inelastic neutron scattering experiments (see Gao et al., 1993); the calculated frequencies are in excellent agreement with the experimental values. The calculated elastic constants for *bcc* Fe (related to the slope of the acoustic branches of the

phonon dispersion curves) are also in a good agreement with experimentally determined values (Vočadlo et al., 1997). More recently, Mao et al. (2001) measured the phonon density of states of Fe up to 153 GPa using nuclear resonant inelastic x-ray scattering. Our calculated phonon density of states for *bcc* Fe at ambient pressure and at 3GPa reported in that paper, are in outstanding agreement with experiment. The agreement with the *hcp* phase is also very good, but less exact than for the *bcc* phase, as our *hcp* simulations were done neglecting magnetic effects. However, nuclear resonant inelastic x-ray scattering gives a very indirect measurement of the phonon density of states, and more research in needed to establish the precision of such high pressure measurements.

The thermal pressure of *hcp* Fe at core conditions has been estimated to be 58 GPa (Anderson, 1995) and 50 GPa (Stixrude et al., 1997); these are in excellent agreement with our calculated thermal pressure for the *hcp* structure (58 GPa at 6000K). By analysing the total pressure as a function of temperature obtained from our calculations for the potential phases of Fe, we were able to ascertain the temperature as a function of volume at two pressures (P=325GPa and P=360GPa) that span the inner core range of pressures. From this we could determine the Gibbs free energy of these structures at those T and P. We found that, on the basis of lattice dynamic calculations over the whole P-T space investigated, the *hcp* phase of Fe has the lowest Gibbs free energy, and is therefore the stable form of Fe under core conditions.

The High P Melting of Fe

Having shown how *ab initio* calculations can be used to establish the sub-solidus phase relations in high P Fe, we turn now to completing the description of the high P/T phase

diagram of Fe, by considering its melting behaviour. An accurate knowledge of the melting properties of Fe is particularly important, as the temperature distribution in the core is relatively uncertain and a reliable estimate of the melting temperature of Fe at the pressure of the inner-core boundary (ICB) would put a much-needed constraint on core temperatures. As with the sub-solidus behaviour of Fe, there appears to be much controversy over its high P melting behaviour (e.g. see Shen and Heinz, 1998). Static compression measurements of the melting temperature, T_m, with the DAC have been made up to ~200 GPa (e.g. Boehler, 1993), but even at lower pressures results for T_m disagree by several hundred Kelvin. Shock experiments are at present the only available method to determine melting at higher pressures, but their interpretation is not simple, and there is a scatter of at least 2000 K in the reported T_m of Fe at ICB pressures (see Nguyen and Holmes, 1999).

Since both our calculations and recent experiments (Shen et al., 1998) suggest that Fe melts from the ε-phase in the pressure range immediately above 60 GPa, we focus here on equilibrium between *hcp* Fe and liquid phases. The condition for two phases to be in thermal equilibrium at a given temperature, T, and pressure, P, is that their Gibbs free energies, G(P, T), are equal. To determine T_m at any pressure, we calculate G for the solid and liquid phases as a function of T and determine where they are equal. In fact, we calculate the Helmholtz free energy, F(V, T), as a function of volume, V, and hence obtain the pressure through the relation $P = -(\partial F/\partial V)_T$ and G through its definition, G = F + PV.

To obtain melting properties with useful accuracy, free energies must be calculated with high precision, because the free energy curves for liquid and solid cross at a shallow angle. It can readily be shown that to obtain T_m with a technical precision of 100 K, non-canceling errors

in G must be reduced below 10 meV. Errors in the rigid-lattice free energy due to basis-set incompleteness and Brillouin-zone sampling are readily reduced to a few meV per atom. In our study, the lattice vibrational frequencies were obtained by diagonalizing the force-constant matrix; this matrix was calculated by our (Alfè, 1998) implementation of the small-displacement method described by Kresse et al. (1995). The difficulty in calculating the harmonic free energy is that frequencies must be accurately converged over the whole Brillouin zone. This requires that the free energy is fully converged with respect to the range of the force-constant matrix. To attain the necessary precision we used repeating cells containing 36 atoms, and to show that such a system gives converged energies, we performed some highly computationally demanding calculations on cells of up to 150 atoms. The anharmonic contributions to the free energy of the solid, and the free energies of the liquid were calculated by molecular dynamics, using thermodynamic integration (Alfè et al., 1999).

To confirm that the methodology can be used accurately to calculate melting temperatures, we have modeled the well studied high P melting behaviour of Al (de Wijs et al., 1998; Vočadlo and Alfè, 2002). Figure 3 shows the excellent agreement that we obtained for this system. In 1999 we published an *ab initio* melting curve for Fe (Alfè et al., 1999). Since the work reported in that paper, we have improved our description of the *ab initio* free energy of the solid, and have revised our estimate of T_m of Fe at ICB pressures to be between 6,200 and 6,350 K (see Fig. 4 and Alfè et al. (2002b,d)). A full analysis of the errors has been reported in Alfè et al. (2002b,d). For pressures P < 200 GPa (the range covered by DAC experiments) our curve lies ~900 K above the experimental values of Boehler (1993) and ~200 K above the more recent values of Shen et al. (1998) (who stress that their values are only a lower bound to T_m). Our curve falls significantly below the shock-based estimates for the T_m of Yoo et al.

(1993), in whose experiments temperature was deduced by measuring optical emission (however, the difficulties of obtaining temperature by this method in shock experiments are well known), but accords almost exactly with the shock data value of Brown and McQueen (1986) and the new data of Nguyen and Holmes (1999).

There are other ways of determining the melting temperature of a system by *ab initio* methods, including performing simulations that model co-existing liquid and crystal phases. The melting temperature of such a system can then be inferred by seeing which of the two phases grows during the course of a series of simulations at different temperatures. This approach was used by Laio et al. (2000) and by Belonoshko et al. (2000) to study the melting of Fe. In their studies they modelled Fe melting using interatomic potentials fitted to *ab initio* surfaces. We discovered, however, that their fitted potentials did not simultaneously describe the energy of the liquid and crystalline phases with the same precision, and so their simulations do not represent the true melting behaviour of Fe, but rather that of the fitted potential. We have recently also used the co-existence method (Alfè et al., 2002d), but with a model potential fitted to our own *ab initio* calculations. Initially, our raw model failed to give the same melting temperature as obtained from our *ab initio* free energy method, but when the results were corrected for the free energy mismatch of the model potential with respect to the *ab initio* energies of liquid and solid, the results for the two methods came into agreement. Thus it would seem as a general principle that there is a way to correct for the shortcomings of model potential co-existence calculations, namely one must calculate the free energy differences between the model and the *ab initio* system for both the liquid and solid phases. This difference in free energy between liquid and solid can then be transformed into an effective temperature correction. When this is done to Belonoshko's data, there is

excellent agreement with our *ab initio* melting curve for Fe (see Fig. 4).

Interestingly we also note that Poirier and Shankland (1993) obtained a value of T_m for Fe at 330 GPa of 6100 ±100 K by using the dislocation melting model, and Anderson (2003) finds a T_m of 5900 ± 300 K on the basis of thermodynamic analysis. Thus with our *ab initio* calculated value of 6200 to 6350 K having been shown to be robust, there now seems to be an emerging consensus on this important melting temperature. Cahn (2001) highlighted that there is still scope for further work on the difficult problem of the modeling of melting, but for the high P melting of Fe at least, it now appears that there may be more problems with reconciling divergent experimental data than there are in obtaining accurate predictions of T_m from *ab initio* studies.

Viscosity of liquid Fe and the Outer Core

The viscosity of high P liquid Fe has been the subject of considerable interest because of its role in determining the dynamics of outer core convection and hence the behaviour of the geodynamo (e.g. see Poirier, 1988). We have reported our investigation into the viscosity, diffusion and thermodynamic properties of Fe in the liquid state in de Wijs et al. (1998) and in Alfè et al. (2000). The technical details of the simulations can be found in these references. In brief, we performed PAW simulations at the 15 thermodynamic states listed in Table 1, all these simulations being done on the 67-atom system. With these simulations, we cover the temperature range 3000-8000 K and the pressure range 60-390 GPa, so that we more than cover the range of interest for the Earth's liquid core. The table reports a comparison of the pressures calculated in the simulations with the pressures deduced by Anderson and Ahrens

(1994) from a conflation of experimental data. In Table 2, we report values for the self diffusion of Fe in liquid Fe, and the viscosity of liquid Fe for the same range of P and T conditions reported above. Since most of the simulations reported in Table 2 are rather short (typically no more than 4 ps) the statistical accuracy on D and η is not great (the error estimates also reported in Table 2). Our *ab initio* simulations demonstrate that under Earth's core conditions liquid Fe is a typical simple liquid. In common with other simple liquids, like liquid Ar and Al, it has a close-packed structure, the coordination number in the present case being ~13. In fact, there appears to be a truly remarkable simplicity in the variation of the liquid properties of Fe with thermodynamic state. For the entire pressure-temperature domain of interest for the Earth's outer core, the diffusion coefficient, D, and viscosity, η, are comparable with those of typical simple liquids, D being $\sim 5 \times 10^{-9}$ $m^2 s^{-1}$ and η being in the range 8-15 mPas, depending on the detailed thermodynamic state. Similar estimates for viscosity of liquid Fe are presented by Stixrude et al. (1998), based on calculations using the tight-binding approximation.

Since the Earth's outer core is in a state of convection, the temperature and density will lie on adiabats. It is straightforward to show that the variation of D and η along adiabats will be rather weak. For example, if we take the data for high-pressure liquid iron compiled by Anderson and Ahrens (1994) then the adiabat for T = 6000 K at the inner core boundary (ICB) pressure 330 GPa has T=4300 K at the core mantle boundary (CMB) pressure of 135 GPa. Taking the densities at these two points from the same source, we find the liquid structure virtually unchanged, apart from a trivial length scaling. For all practical purposes, then, it can be assumed that variation of thermodynamic conditions across the range found in the core has almost no effect on the liquid structure. For the same reasons, the diffusion

coefficient D and viscosity also show little variation, so that the diffusion coefficient D is $5\pm0.5\times10^{-9}$ m^2s^{-1} without significant variation as one goes from ICB to CMB pressures along the adiabat, and in parallel η goes from 15±5 to 8.5 ±1 mPas. Similar values were established from empirical scaling relations (Poirier, 1988), and further *ab initio* calculations and experimental studies of viscosity in liquid Fe-S (Dobson et al, 2000; Urakawa et al, 2001) suggest a very slight effect of sulphur on viscosity. Thus, it seems that these calculations finally resolve the issue of the viscosity of the outer core, which historically was considered to be uncertain to within ~12 orders of magnitude (e.g., Poirier, 1988; Secco, 1995)! A low viscosity has important implications for the geodynamic description of the outer core. The nonlinear equations of magnetohydrodynamics cannot be solved exactly, and simplified linear approximations are often used. Depending on these approximations, contributions to the forces acting on the fluid in the outer core, such as Coriolis, Lorentz and viscous, may be treated as small or negligible. The relative importance of the viscous and Coriolis forces is characterized by the Ekman number, given by $Ek = \eta/(\rho\Omega L^2)$, where ρ is the fluid density, Ω is the Earth's rotational velocity, and L is the fluid thickness. Our calculations suggest $Ek \sim 4\times10^{-15}$, indicating that viscous forces are indeed negligible when compared with the Coriolis force. This supports models based on the assumption that the viscosity of the core is negligible, and favours a picture in which the core is in a state of small-circulation turbulent convection, in contrast to models having a viscosity of $\sim10^7$ Pa which imply a coherent pattern on a much larger scale, comparable with the core radius.

The Composition and Temperature of the Core

As discussed above, on the basis of seismology and data for pure Fe it is considered that the

outer and inner core contain some light element impurities. Cosmochemical abundances of the elements, combined with models of the Earth's history, limit the possible impurities to a few candidates. Those most often discussed are S, O and Si (e.g. Poirier, 1994b; Allègre et al., 1995; McDonough and Sun, 1995), and we have to date confined our studies to these three. Our strategy for constraining the impurity fractions and the temperature of the core is based on the supposition that the solid inner core is slowly crystallising from the liquid outer core, and that therefore the inner and outer core are in thermodynamic equilibrium at the ICB. This implies that the chemical potentials of Fe and of each impurity must be equal on the two sides of the ICB.

If the core consisted of pure Fe, equality of the chemical potential (Gibbs free energy in this case) would tell us only that the temperature at the ICB is equal to the melting temperature of Fe at the ICB pressure of 330 GPa. With impurities present, equality of the chemical potentials for each impurity element imposes a relation between the mole fractions in the liquid and the solid, so that with S, O and Si we have three such relations. But these three relations must be consistent with the accurate values of the mass densities in the inner and outer core deduced from seismic and free-oscillation data. We outline below our recent finding (Alfè et al., 2002c) that *ab initio* results for the densities and chemical potentials in the liquid and solid Fe/S, Fe/O and Fe/Si alloys determine with useful accuracy the mole fraction of O and the sum of the S and Si mole fractions in the outer and inner core, as well as enabling us to determine the temperature at the ICB.

The chemical potential, μ_x, of a solute X in a solid or liquid solution is conventionally expressed as $\mu_x = \mu_x^0 + k_B T \ln a_x$, where μ_x^0 is a constant and a_x is the activity. It is common

practice to write $a_x = \gamma_x c_x$, where γ_x is the activity coefficient and c_x the concentration of X. The chemical potential can therefore be expressed as:

$$\mu_x = \mu_x^0 + k_B T \ln \gamma_x c_x \tag{6}$$

which we rewrite as:

$$\mu_x = \mu_x^* + k_B T \ln c_x \tag{7}$$

It is helpful to focus on the quantity μ_x^* for two reasons: first, because it is a convenient quantity to obtain by *ab initio* calculations (Alfè et al., 2002c); second, because at low concentrations the activity coefficient, γ_x, will deviate only weakly from unity by an amount proportional to c_x, and by the properties of the logarithm the same will be true of μ_x^*.

The equality of the chemical potentials μ_x^l and μ_x^s in coexisting liquid and solid (superscripts 1 and s respectively) then requires that:

$$\mu_x^{*l} + k_B T \ln c_x^l = \mu_x^{*s} + k_B T \ln c_x^s \tag{8}$$

or equivalently

$$c_x^s / c_x^l = \exp\left[(\mu_x^{*l} - \mu_x^{*s}) / k_B T\right] \tag{9}$$

This means that the ratio of the mole fractions c_x^s and c_x^l in the solid and liquid solution is determined by the liquid and solid thermodynamic quantities μ_x^{*l} and μ_x^{*s}. Although liquid-solid equilibrium in the Fe/S and Fe/O systems has been experimentally studied up to pressures of around 60 GPa, there seems little prospect of obtaining experimental data for μ_x^{*l} - μ_x^{*s} for Fe alloys at the much higher ICB pressure. However, we have shown (Alfè et al., 2002c) recently that the fully *ab initio* calculation of μ_x^{*l} and μ_x^{*s} is technically feasible. Thus, the chemical potential, μ_x, of chemical component X can be defined as the change of Helmholtz free energy when one atom of X is introduced into the system at constant temperature T and volume V. In *ab initio* simulations, it is awkward to introduce a new atom, but the awkwardness can be avoided by calculating μ_x^* - μ_{Fe}^*, which is the free energy change, ΔF, when an Fe atom is replaced by an X atom. For the liquid, this ΔF is computed by applying the technique of 'thermodynamic integration' to the (hypothetical) process in which an Fe atom is continuously transmuted into an X atom. We have recently performed such calculations for transmuting Fe atoms into S, O and Si (Alfè et al., 2002a).

The full technical details of our simulations are given in Alfè et al. (2000, 2002c), but in brief, they were performed at constant volume and temperature on systems of 64 atoms; the duration of the simulations after equilibration was typically 6 ps in order to reduce statistical errors to an acceptable level; the number of thermodynamic integration points used in transmuting Fe into X was 3, and we carefully checked the adequacy of these numbers of points. Our results reveal a major qualitative difference between O and the other two impurities. For S and Si, μ_x^* is almost the same in the solid and the liquid, the differences being at most 0.3 eV, i.e. markedly smaller than $k_BT \sim 0.5$ eV; but for O the difference of μ_x^* between solid and liquid is ~ 2.6 eV, which is much bigger than k_BT. This means that added

O will partition strongly into the liquid, but added S or Si will have similar concentrations in the two phases.

Our simulations of the chemical potentials of the alloys can be combined with simulations of their densities to investigate whether the known densities of the liquid and solid core can be matched by any binary Fe/X system, with X = S, O or Si. Using our calculated partial volumes of S, Si and O in the binary liquid alloys, we find that the mole fractions required to reproduce the liquid core density are 16, 14 and 18 % respectively (Fig. 5, panel (a) displays our predicted liquid density as a function of c_x compared with the seismic density). Our calculated chemical potentials in the binary liquid and solid alloys then give the mole fractions in the solid of 14, 14 and 0.2 % respectively that would be in equilibrium with these liquids (see Fig. 5, panel (b)). Finally, our partial volumes in the binary solids give ICB density discontinuities of 2. 7+/-0.5, 1.8+/-0.5 and 7.8+/-0.2 % respectively (Fig. 5, panel (c)). As expected, for S and Si, the discontinuities are considerably smaller than the known value of 4.5+/-0.5 %; for O, the discontinuity is markedly greater than the known value. We conclude that none of the binary systems can account for the discontinuity quantitatively. However, it clearly can be accounted for by O together with either or both of S and Si. *Ab initio* calculations on general quaternary alloys containing Fe, S, O and Si will clearly be feasible in the future, but currently they are computationally too demanding, so for the moment we assume that the chemical potential of each impurity species is unaffected by the presence of the others. Our estimated mole fractions needed to account for the ICB density discontinuity, were reported in Alfè et al. (2002a) as being 8.5±2.5 mole % S/Si and 0.2±0.1 % O in the inner core and 10±2.5 % S/Si and 8±2.5 % O in the liquid outer core. This compositional estimate was based on the value of the density discontinuity at the ICB

determined by Shearer and Masters (1990). Since then, Masters and Gubbins (2003) have reassessed the free oscillation data set, and have determined the density jump at the ICB to be 0.82±0.18 Mg m^{-3}, which is larger than the previous estimates. Using the new density data of Masters and Gubbins (2003) leads to a revised core composition of 7±2.5 mole % S/Si and 0.2±0.1 % O for the inner core and 8±2.5 % S/Si and 13±2.5 % O for the outer core. This change in our estimate of core composition emphasises the need for very accurate seismic data if we wish to constrain more precisely the composition of the core.

With the calculated impurity chemical potentials, we can use the Gibbs-Duhem relation to compute the change in the Fe chemical potential caused by the impurities in the solid and liquid phases (Alfè et al., 2002a). By requiring the chemical potential of Fe to be the same in both phases, we obtained the change, ΔT, of melting temperature relative to that of pure Fe. Our estimate for ΔT is between -700 and -800 K, depending upon the value of the density contrast at the ICB. Using our own *ab initio* estimate of the melting temperature of pure Fe at core pressure, we predict that the Earth's temperature at the ICB to be between 5400 and 5650 K. Interestingly, this is very close to the value recently inferred by Steinle-Neumann et al. (2001) from independently determined *ab initio* calculations on the elastic properties of the inner core.

Using our calculated values for the ICB temperature, and our *ab initio* values for the Grüneisen parameter, γ, for liquid Fe only the outer core adiabat (Vočadlo et al., 2003), it is possible to determine the core temperature at the core mantle boundary from the relation defining the adiabatic temperature gradient:

$$\partial T/\partial r = -\gamma g T/\Phi \quad (10)$$

where Φ is the seismic parameter and g is the acceleration due to gravity. Like Anderson (2003), we find γ to be ~1.5 and virtually constant in the outer core, which leads to our entirely *ab initio* estimate of the core temperature at the CMB of between 3950 and 4200K. Again, this range is in excellent agreement with that inferred from thermodynamic arguments (Anderson, 2003).

Possible Structure of the Inner Core

The conventional interpretation of the origin of the seismic anisotropy of the inner core is based on the idea of the development of partial alignment of the elastically anisotropic crystals of *hcp* Fe (e.g. Song, 1997). The static elastic constant of *hcp* Fe were first calculated by Stixrude and Cohen (1995) and then by Söderlind et al. (1996). The low temperature elastic constants of *hcp* Fe at 39 and 211 GPa were measured in an experiment reported by Mao et al (1999). The overall the agreement between the experimental and various *ab initio* studies are excellent, and the measured and calculated bulk and shear moduli and the seismic velocities of *hcp* Fe as a function of pressure are shown in Figs 6 and 7. The calculated values compare well with experimental data at higher pressures, but discrepancies at lower pressures are probably due to the neglect of magnetic effects in the simulations (see also the discussion in Steinle-Neumann et al., 2003).

The effect of temperature on the elastic constants of Fe was reported by Steinle-Neumann et al. (2001) based on calculations using the approximate "particle in a cell" method. They

found a significant change in the c/a ratio of the *hcp* structure with temperature, which causes a marked reduction in c_{33}, c_{44} and c_{66} with increasing temperature. This led them to conclude that increasing temperature reverses the sense of the single crystal longitudinal anisotropy of *hcp* Fe, and that the anisotropy of the core should now be viewed as being due to *hcp* Fe crystals having their c-axis preferably aligned equatorially, rather than axially as originally suggested by Stixrude and Cohen (1995). However, the *ab initio* determination of high T elastic constants is very taxing and is far from routine. In fact, Oganov et al. (2001) were the first to calculate entirely *ab initio* (using AIMD) the high T elastic constants of any mineral, and further work is needed to confirm the high T properties of *hcp* Fe. Our calculations (Gannarelli et al., 2003) have failed thus far to reproduce the strong effect of temperature on c/a seen by Steinle-Neumann et al., and if this result is confirmed by more precise molecular dynamic simulations, then it will have important implications for the interpretation of the seismic tomography of the inner core.

The nature of inner core anisotropy has recently been shown to be more complex than previously thought, and Beghein and Trampert (2003) have shown that free oscillation data cannot be simply interpreted in terms of the elastic properties of *hcp* Fe as reported by Steinle-Neumann et al. (2001). Furthermore, the assumption that *hcp* Fe is the thermodynamically stable polymorph of Fe at the high temperatures found in the inner-core has also been recently questioned (Brown, 2001). In spite of the arguments in favour of *hcp* Fe, it has been proposed by a number of workers that *bcc* Fe might be the stable high P/T phase (Ross et al, 1990; Matsui and Anderson, 1997). A strong argument in favour of the stability of *bcc* Fe under these conditions is that a number of transition metals (e.g. Ti, Zr..) are known to transform from close-packed structures to the *bcc* structure at temperatures just

below their melting curve. However, until recently it appeared that theoretical calculations had ruled out the *bcc* structure as a candidate for the stable phase of Fe in the core. As reviewed in for example Steinle-Neumann et al. (2003) this was because *ab initio* calculations have shown that the *bcc* structure becomes elastically unstable at pressures above ~150 GPa, and that the enthalpy of the perfect *bcc* structure is considerably higher than that of the *hcp* phase. However, these arguments are not conclusive because they are based on athermal or lattice dynamical *ab initio* calculations, which because of the dynamical instability of *bcc* Fe cannot be used to determine entropic effects at high pressures. In the past, computing limitations prevented a more sophisticated analysis, but recent methodological developments mean that it is now possible accurately to address these thermal effects. Thus, to resolve the controversy over the effect of temperature on the stability of *bcc* Fe, we recently performed the very first *ab initio* molecular dynamics (AIMD) calculations on *bcc* Fe to simulate directly its behaviour at the high temperatures relevant to the Earth's inner core (Vočadlo et al, 2003).

In order to establish whether the *bcc* phase at high pressure is entropically stabilised by temperature, we performed AIMD at 6000K for a chosen volume of 7.2 $Å^3$ per atom (~core density) and compared the results with those from simulations performed at lower temperatures. The stability of the *bcc* structure at high temperatures was assessed in four separate ways: (i) the anisotropic stresses were analysed for evidence of elastic stability, (ii) the atomic positions with respect to those in a perfect *bcc* structure were analysed for evidence of vibrational stability, (iii) the structure factors were calculated to help identify the phases present, (iv) the relative free energy with respect to the *hcp* structure was calculated in order to determine its thermodynamic stability at core conditions. The graph shown in the

upper left corner of Fig. 8 gives the six components of the stress tensor of the cubic *bcc* cell at 6000K as a function of simulation time; it can be seen that the supercell experiences hydrostatic stresses throughout the simulation, suggesting that the cell is stable. It is clear that when the temperature is considerably reduced (to below 3000K), the cell is no longer under hydrostatic stress indicating that the *bcc* Fe structure is no longer elastically stable.

In order to identify whether the atoms in our simulation cell have moved away from the perfect *bcc* structure, we can look at the positions of the atoms throughout the simulation relative to *bcc* lattice sites. A convenient method for analysing the evolution of the atomic positions over the length of the simulation is to use the position correlation function, p(t), which not only tells us where the atoms are, but also may indicate the existence of an imminent phase transition. The graph in the lower left corner of Fig. 8 shows p(t) at 6000K; it is clear that $p(t) \rightarrow 0$ as $t \rightarrow \infty$, indicating that the atomic positions in the simulation cell are, on average, those of a perfect *bcc* structure. We can therefore conclude that, at 6000K and a volume of 7.2 $Å^3$ per atom (~core pressures and temperatures), the *bcc* structure is vibrationally stable. However, as the system is cooled, it can readily be seen that the atoms deviate significantly and permanently away from a *bcc* structure (i.e., $p(t) \neq 0$ as $t \rightarrow \infty$) below 3000K. In fact, analysis of the structure factors (not presented) show that the *bcc* phase undergoes a transition to the *omega* phase (Vočadlo et al., 2003).

Having established that the *bcc* phase under pressure is elastically and vibrationally stable at high temperatures, we need to calculate its free energy at core conditions to determine its thermodynamic stability with respect to *hcp*. We used the method of thermodynamic integration (Vočadlo et al., 2003) which allows us to calculate the difference in free energy,

$F-F_0$, between our *ab initio bcc* system and a reference system whose potential energies are U and U_0 respectively. As mentioned above, we have successfully used this method to calculate *ab initio* the melting behaviour of Al at pressure, and the properties of liquid and *hcp* Fe. An important point to note is that our calculations on *bcc* Fe were performed *without* spin polarisation. It is well known that the *bcc* phase has a significant magnetic moment at core pressures (Söderlind et al., 1996) which, if maintained at high temperature, would contribute to the free energy through the disordering of the orientations of the spins. However, at high temperatures, the magnetic moment will be destroyed by thermal excitation of the electrons. We performed calculations on the *bcc* structure at inner core pressures as a function of electronic temperature (2000-6000K). Our results show that, as expected, the magnetic moment decreases with temperature, and disappears altogether well before core temperatures are reached; there is, therefore, no contribution to the free energy of *bcc* Fe from magnetic entropy.

Table 3 shows our calculated Helmholtz free energies for the *bcc* and *hcp* phases over a range of volumes and temperatures along (and below) our previously determined melting curve of *hcp* Fe. It is clear that in all cases $F_{bcc} > F_{hcp}$. However, the differences in free energies are small (33-58 meV/atom along T_m). The Earth's inner core, however, is known not to be made of pure Fe, but is expected to be alloyed with between 5 to 10 mol% of a lighter element. It is now reasonably well established that either separately or together S and Si are two of the most probable light elements alloyed with Fe in the core (Poirier, 1994a; Allègre et al., 1995). Additionally, recent experiments (Dobson et al., 2002) have shown that at high pressures FeSi crystallises with the CsCl-structure (i.e. has identical atomic co-ordinates to *bcc*-Fe), and at lower concentrations Si stabilises *bcc* Fe under pressure and temperature

conditions at which pure Fe is found with the *hcp* structure (Lin et al., 2002; Dubrovinsky et al., 2003). We therefore investigated the energetic effect of the substitution of S and Si in *bcc* and *hcp*-Fe at representative core cell volumes (7.2 $Å^3$). We find that the enthalpies of the S and Si defects are respectively 1.4 and 1.2 eV per defect atom more stable in the *bcc* structure than in the *hcp* phase. Therefore, for example, a 5 mol% concentration of Si in Fe, would stabilise the *bcc* phase by 60 meV. Thus, we conclude that the presence of S or Si as the light impurity element in the core, at appropriate concentrations, could favour the formation of a *bcc*- rather than an *hcp*-structured Fe alloy phase at temperatures just below T_m at inner core pressure. If this is the case, it suggests that presence of a *bcc*-structured alloy must be a strong candidate for explaining the observed seismic complexity of the inner core recently reported by Beghein and Trampert (2003).

Conclusion

The past decade has seen a major advance in the application of *ab initio* methods in the solution of high pressure and temperature geophysical problems, thanks to the rapid developments in high performance computing. We are now in a position to calculate from first principles the free energies of solid and liquid phases, and hence to determine both the phase relations and the physical properties of planetary forming phases. *Ab initio* methods have enabled us to calculate that the ICB temperature is between 5400 and 5650K and that the core temperature at the CMB is 3950 to 4200K. We also now know that the outer core has a viscosity of $\sim 10^{-2}$ Pas. The composition of the core can be determined, but estimates are very sensitive to the seismologically inferred values of core density. With the clearer insight that *ab initio* modelling gives our understanding of the physical, chemical and thermal

properties of the core, it is now becoming possible develop more accurate descriptions of the geodynamo and the evolution of the Earth's magnetic field (see for example Gubbins et al., 2003).

The high P and T structure and elastic properties of Fe and its alloys are still the subject of some controversy, but theory should soon be able to resolve the issue. In the future, we look forward to the advent of routinely available 'terascale' computing. This will open new possibilities for geophysical modelling. We will be able to model more complex and larger systems, to investigate for example solid state rheological problems, or physical properties such as thermal and electrical conductivity, and to model the possible chemical processes occurring at the CMB. However, we recognise that the DFT methods we currently use are still approximate, and fail for example to describe the band structure of important phases such as FeO. In the future we will need to consider using terascale facilities to implement more demanding but more accurate techniques, such as those based on quantum Monte Carlo methods.

Acknowledgements

DA and LV are supported by Royal Society University Research Fellowships. MJG thanks GEC and Daresbury Laboratory for their support. Our work reported in this paper was supported by NERC grants GR3/12083 and GR9/03550. The calculations were run on the Cray T3D and Cray T3E machines at Edinburgh and the Manchester CSAR Centre, and on the Origin 2000 machine at the UCL HiPerSPACE Centre.

References

Alfè, D., 1998. Program available from, http://chianti.geol.ucl.ac.uk/~dario/phon.tar.z

Alfè, D., Gillan, M.J., and Price, G.D., 1999. The melting curve of iron at the pressures of the Earth's core from *ab initio* calculations. Nature, 401: 462-464.

Alfè, D., Gillan, M.J., and Price, G.D., 2002a. Composition and temperature of the Earth's core constrained by combining *ab initio* calculations and seismic data. Earth Planet. Sci. Lett., 195: 91-98.

Alfè, D., Gillan, M.J., and Price, G.D., 2002c. *Ab initio* chemical potential of solid and liquid solutions and chemistry of the Earth's core. J. Chemical Physics. 116: 7127-7136.

Alfè, D., Gillan, M.J., and Price, G.D., 2002d. Complementary approaches to the *ab initio* calculation of melting properties. J. Chemical Physics. 116: 6170-6177.

Alfè, D., Kresse, G., and Gillan, M.J., 2000. Structure and dynamics of liquid Iron under Earth's core conditions. Physical Review . 61: 132-142.

Alfè, D., Price, G.D., and Gillan, M.J., 2001. Thermodynamics of hexagonal-close-packed iron under Earth's core conditions. Physical Review. B64: 045123.

Alfè, D., Price, G.D., and Gillan, M.J., 2002b. Iron under Earth's core conditions: Liquid-state thermodynamics and high-pressure melting curve from *ab initio* calculations. Phys. Review. B65: 165118, 1-11.

Allègre, C.J., Poirier, J.P., Humler, E., and Hofmann, A.W., 1995. The chemical composition of the Earth. Phys. Earth Planet. Interiors. 134: 515-526.

Allen, M.P., and Tildesley, D.J., 1987. Computer Simulation of Liquids. Oxford University Press, Oxford, UK.

Anderson, O.L., 1995. Equations of state of solids for Geophysics and ceramic science. Oxford

University Press, Oxford, UK.

Anderson, O.L., 2003. The three-dimensional phase diagram of iron. In: Earth's Core (eds. V. Dehant, K.C. Creager, S-i. Karato, S. Zatman). AGU, Geodynamics Series, 31, 83-104.

Anderson, W.W., and Ahrens, T.J., 1994. An equation of state for liquid iron and implication for the Earth's core. J. Geophys. Res. 99: 4273-4284.

Andrault, D., Fiquet, G., Kunz, M., Visocekas, F., and Häusermann, D., 1997. The orthorhombic structure of iron: an in situ study at high temperature and high pressure. Science. 278: 831-834.

Beghein, C., and Trampert, J., 2003. Robust Normal Mode Constraints on Inner-Core Anisotropy from Model Space Search. Science, 299, 552-555.

Belonoshko, A.B., Ahuja, R., and Johansson, B., 2000. Quasi- *ab initio* molecular dynamic study of Fe melting. Phys Rev Lett. 84: 3638-3641.

Birch, F., 1964. Density and composition of mantle and core. J Geophys Res, 69, 4377-4388.

Blöchl, P. E., 1994. Projector augmented-wave method. *Phys. Rev. B* **50**, 17953-17979.

Boehler, R., 1993. Temperature in the Earth's core from the melting point measurements of iron at high static pressures. Nature. 363: 534-536.

Boehler, R., 2000. High-pressure experiments and the phase diagram of lower mantle and core materials. Reviews of Geophys. 38: 221-245.

Born, M., and Huang, K., 1954. Dynamical Theory of Crystal Lattices. Oxford University Press, Oxford, UK.

Birch, F., 1952. Elasticity and the constitution of the Earth's interior. J Geophys. Res. 57: 227-286.

Brown, J.M., 2001. The equation of state of Iron to 450GPa: another high pressure solid phase? Geophys Res. Letts. 28: 4339-4342.

Brown, J.M., and McQueen, R.G., 1986. Phase transitions, Grüneisen parameter and elasticity for shocked iron between 77 GPa and 400 GPa. J. Geophys. Res. 91: 7485-7494.

Cahn, RW (2001) Melting from within. Nature, 413, 582-3.

Car, R., and Parrinello, M., 1985. Unified Approach for Molecular Dynamics and Density Functional Theory. Phys. Rev. Lett. 55: 2471-2474.

Creager, K.C., 1992. Anisotropy of the inner core from differential travel times of the phases PKP and PKIKP. Nature, 356, 309-314.

Dobson, D.P., Crichton, W.A., Vocadlo, L., Jones, A.P., Wang, Y.B., Uchida, T., Rivers, M., Sutton, S., and Brodholt, J.P., 2000. In situ measurement of viscosity of liquids in the Fe-FeS system at high pressures and temperatures. American Mineralogist, 85, 1838-1842.

Dobson, D.P., Vočadlo, L., and Wood, I.G., 2002. A new high-pressure phase of FeSi. Amer. Mineral. 87, 784-787.

Dubrovinsky, L., Dubrovinskaia, N., Langenhorst, F., Dobson, D., Rubie, D., Gessmann, C., Abrikosov, I.A., Johansson, B., Baykov, V.I., Vitos, L., Le Bihan, T., Crichton, W.A., Dmitriev, V., and Weber, H.P., 2003. Iron-silica interaction at extreme conditions and the electrically conducting layer at the base of Earth's mantle. Nature, 422, 58-61.

Dziewonski, A.M., and Gilbert, F., 1971. Solidity of the inner core of the Earth inferred from normal mode observations. Nature, 234, 465-466.

Fiquet, G., Badro, J., Guyot, F., Requardt, H., and Krisch, M., 2001. Sound velocities in iron to 110 gigapascals. Science, 291, 468-47.

Gannarelli, C.M.S., Alfè, D., and Gillan, M.J. (2003) The particle-in-cell model for ab initio thermodynamics: implications for the elastic anisotropy of the Earth's inner core. Phys. Earth Planet. Interiors, Submitted.

Gao, F., Johnston, R.L., and Murrell, J.N., 1993. Empirical many-body potential energy

functions for Iron. J. Phys. Chem. 97: 12073-12082.

Gillan, M.J., 1997. The virtual matter laboratory. Contemp. Phys. 38: 115-130.

Gubbins, D., Alfè, D., Masters, G., Price, G.D., and Gillan, M.J., 2003. Can the Earth's dynamo run on heat alone? Geophys. J. Int. In press.

Ishii, M., and Dziewonski, A.M., 2002. The innermost inner core of the earth: Evidence for a change in anisotropic behaviour at the radius of about 300 km. Proceedings of the National Academy Of Sciences Of The United States Of America . 99: 14026-14030.

Kresse, G., Furthmüller, J., and Hafner, J., 1995. Ab-initio force-constant approach to phonon dispersion relations of diamond and graphite. Europhys. Lett. 32: 729-734.

Kresse, G., and Furthmüller, J., 1996. Efficient iterative schemes for ab-initio total-energy calculations using a plane-wave basis set. Phys. Rev. B54: 11169-11186.

Laio, A., Bernard, S., Chiarotti, G.L., Scandolo, S., and Tosatti, E., 2000. Physics of iron at Earth's core conditions. Science. 287: 1027-1030.

Lin, J-F., Heinz, D. L., Campbell, A. J., Devine, J. M., and Shen, G., 2002. Iron-silicon alloy in Earth's core? Science 295, 313-315.

Mao, H.K., Shu, J., Shen, G., Hemley, R.J., Li, B., and Sing, A.K., 1999. Elasticity and rheology of iron above 220GPa and the nature of the Earth's inner core. Nature. 399: 280.

Mao, H.K., Xu, J., Struzhkin, V.V., Shu, J., Hemley, R.J., Sturhahn, W., Hu, M.Y., Alp, E.E., Vočadlo, L., Alfè, D., Price, G.D., Gillan, M.J., Schwoerer-Bohning, M., Hausermann, D., Eng, P., Shen, G., Giefers, H., Lubbers, R., and Wortmann, G., 2001. Phonon density of states of iron up to 153 gigapascals. Science. 292: 914-916.

Masters, G., and Gubbins, D., 2003. On the resolution of density within the Earth. Geophys. J. Int., in press.

Matsui, M., and Anderson, O.L., 1997. The case for a body-centered cubic phase for iron at

inner core conditions. Physics Earth Planetary Interiors. 103: 55-62.

McDonough, W.F., and Sun, S.-S., 1995. The composition of the Earth. Chem. Geol. 120: 223-253.

Nguyen, J.H., and Holmes, N.C., 1999. Iron sound velocities in shock wave experiments. Shock Compression of Condensed Matter. CP505: 81-84.

Oganov, A.R., Brodholt, J.P., Price, G.D., 2001. The elastic constants of $MgSiO_3$ perovskite at pressures and temperatures of the Earth's mantle. Nature, 411, 934- 937

Parker, S.C., and Price, G.D., 1989. Computer Modelling of Phase Transitions in Minerals. Advances in Solid State Chemistry. 1: 295-327.

Parrinello, M., and Rahman, A., 1980. Crystal Structure and Pair Potentials: A Molecular Dynamics Study. Phys. Rev. Lett. 45: 1196-1199.

Poirier, J.P., 1988. Transport-Properties Of Liquid-Metals And Viscosity Of The Earths Core. Geophys. J. Int., 92, 99-105.

Poirier, J.P., 1994a. Light elements in the Earth's outer core: A critical review. Phys. Earth Planet. Inter. 85: 319-337.

Poirier, J.P., 1994b. Physical-properties of the Earths core. Cr. Acad. Sci. II. 318: 341-350.

Poirier, J.P., and Shankland, T.J., 1993. Dislocation Melting Of Iron And The Temperature Of The Inner-Core Boundary, Revisited. Geophys. J. Int., 115, 147-151.

Ross, M., Young, D. A., and Grover, R., 1990. Theory of the iron phase diagram at Earth core conditions. J. Geophys. Res. **95**, 21,713-21,716.

Saxena, S.K., Dubrovinsky, L.S., and Häggkvist, P., 1996. X-ray evidence for the new phase of β-iron at high temperature and high pressure. Geophys. Res. Lett. 23: 2441-2444.

Secco, R.A., 1995. Viscosity of the Outer Core. In:Mineral Physics and Crystallography: A handbook of physical constants. AGU Reference Shelf 2 (ed T.J. Ahtens). 218-226.

Shearer, P.M., and Masters, G., 1990. The density and shear velocity contrast at the inner core boundary. Geophys. J. Int., 102, 491-498.

Shen, G.Y., and Heinze, D.L., 1998. High Pressure melting of deep mantle and core materials. In: Ultrahigh-pressure Mineralogy (ed. R.J. Hemley). Reviews in Mineralogy. 37: 369-398.

Shen, G.Y., Mao, H.K., Hemley, R.J., Duffy, T.S., and Rivers, M.L., 1998. Melting and crystal structure of iron at high pressures and temperatures. Geophys. Res. Lett. 25: 373.

Söderlind, P., Moriarty, J.A., and Wills, J.M., 1996. First-principles theory of iron up to earth-core pressures: Structural, vibrational and elastic properties. Phys. Rev. B53:14063-14072.

Song, X.D., 1997. Anisotropy of the Earth's Inner core. Reviews Geophys., 35, 297-313.

Song, X. D., and Helmberger, D. V., 1998. Seismic evidence for an inner core transition zone. Science, **282**, 924-927.

Steinle-Neumann, G., Stixrude, L., and Cohen, R.E., 1999. First-principles elastic constants for the *hcp* transition metals Fe, Co, and Re at high pressure. Phys. Rev. B60: 791-799.

Steinle-Neumann, G., Stixrude, L., and Cohen, R.E., 2003. Physical properties of iron in the inner core. In: Earth's Core (eds. V. Dehant, K.C. Creager, S-i. Karato, S. Zatman). AGU, Geodynamics Series, 31, 137-162.

Steinle-Neumann, G., Stixrude, L., Cohen, R.E., and Gülseren, O., 2001. Elasticity of iron at the temperature of the Earth's inner core. Nature. 413: 57-60.

Stixrude, L., and Brown, J.M., 1998. The Earth's Core. In: Ultrahigh-pressure Mineralogy (ed. R.J. Hemley). Reviews in Mineralogy. 37: 261-283.

Stixrude, L., and Cohen, R.E., 1995. Constraints on the Crystalline Structure of the Inner Core - Mechanical Instability of *bcc* Iron at High-Pressure. Geophys. Res. Lett. 22: 125-128.

Stixrude, L., Cohen, R.E., and Hemley, R.J., 1998. Theory of minerals at high pressure. In:

Ultrahigh-pressure Mineralogy (ed. R.J. Hemley). Reviews in Mineralogy. 37: 639-671.

Stixrude, L., Wasserman, E., and Cohen, R.E., 1997. Composition and temperature of the Earth's inner core. J Geophys. Res. 102: 24729-24739.

Urakawa S, Terasaki, H., Kato, T.,2001.The effect of temperature, pressure, and sulfur content on viscosity of the Fe-FeS melt.Earth Planet. Sc. Lett., 190, 93-101.

Vočadlo, L., and Alfè, D., 2002. The *ab initio* melting curve of aluminum. Phys. Rev. B65: 214105, 1-12.

Vočadlo, L., Alfè, D., Gillan, M.J., Wood, I.G., Brodholt, P.J., and Price, G.D., 2003. Possible thermal and chemical stabilisation of body- centred- cubic iron in the Earth's core? Nature, in press.

Vočadlo, L., Brodholt, J., Alfè, D., Price, G.D., and Gillan, M.J., 1999. The structure of iron under the conditions of the Earth's inner core. Geophys. Res. Lett. 26: 1231-1234.

Vočadlo, L., deWijs, G.A., Kresse, G., Gillan, M.J., and Price, G.D., 1997. First principles calculations on crystalline and liquid iron at Earth's core conditions. Faraday Discussions. 106: 205-217.

Wasserman, E., Stixrude, L., and Cohen, R.E., 1996. Thermal properties of iron at high pressures and temperatures. Phys. Rev. B53: 8296-8309.

de Wijs, G.A., Kresse, G., and Gillan, M.J., 1998. First order phase transitions by first principles free energy calculations: The melting of Al. Phys. Rev. B57: 8233-8234.

Yoo, C.S., Holmes, N.C., Ross, M., Webb, D.J., and Pike, C., 1993. Shock temperatures and melting of iron at Earth core conditions. Phys. Rev. Lett. 70: 3931-3934.

Table 1. Pressure (in GPa) calculated as a function of temperature (T) and density for liquid Fe. Experimental estimates are in parenthesis, from Anderson and Ahrens (1994).

	ρ (kg m^{-3})				
T (K)	9540	10 700	11 010	12 130	13 300
3000	60				
4300		132 (135)			
5000		140 (145)			
6000	90	151 (155)	170 (170)	251 (240)	360 (335)
7000		161	181	264 (250)	375 (350)
8000		172	191	275	390 (360)

Table 2. The diffusion coefficient (D) and the viscosity (η) from our *ab initio* simulations of liquid Fe at a range of temperatures and densities. The error estimates come from statistical uncertainty due to the short duration of the simulations.

		ρ (kg m^{-3})				
	T (K)	9540	10 700	11 010	12 130	13 300
D (10^{-9} m^2 s^{-1})	3000	4.0±0.4				
	4300		5.2±0.2			
	5000		7.0±0.7			
	6000	14±1.4	10±1	9±0.9	6±0.6	5±0.5
	7000		13±1.3	11±1.1	9±0.9	6±0.6
η (mPa s)	3000	6±3				
	4300		8.5±1			
	5000		6±3			
	6000	2.5±2	5±2	7±3	8±3	15±5
	7000		4.5±2	4±2	8±3	10±3

Table 3: The *ab initio* Helmholtz free energy per atom of the *bcc* and *hcp* phases of Fe at state points along (*and below) the calculated melting curve. In this work, the reference system is a simple inverse power potential which takes the form $U=4\varepsilon(\Gamma/r)^{\alpha}$ where ε=1 eV, Γ=1.77 Å, α=5.86. We have previously shown that this reference potential, based on only a repulsive term, describes the *ab initio* system extremely well; the bonding term is almost independent of the atomic positions, depending only on the volume and temperature of the system. We stress, however, that the final result is totally independent of the choice of reference system. We performed these calculations on a 64 atom supercell (4x4x4 primitive cells) with a 3x3x3 **k**-point grid. Considerable effort was spent on convergence tests in **k**-point sampling to reduce the error in free energies to <10 meV per atom. Cell size effects have been extensively studied in our previous work *hcp*-Fe (Alfè et al., 2001).

V (Å^3)	**T (K)**	**F_{bcc} (eV)**	**F_{hcp} (eV)**	**$DF_{bcc-hcp}$ (meV)**
9.0	3500	-10.063	-10.109	46
8.5	3500	-9.738	-9.796	58
7.8	5000	-10.512	-10.562	50
7.2	6000	-10.633	-10.668	35
6.9	6500	-10.545	-10.582	37
6.7	6700	-10.288	-10.321	33
***7.2**	3000	-7.757	-7.932	175

Figure Captions

Fig 1. A hypothetical phase diagram for Fe, incorporating all the experimentally suggested high P/T phase transformations. Our calculations suggest that the phase diagram is in fact much more simple than this, with *hcp* Fe being the only high P/T phase stable at core pressures.

Fig 2. The phonon dispersion curves along a ΓHΓN path in reciprocal space for *bcc* Fe. The solid lines are from our calculations, and the open circles are experimental points reported in Gao et al. (1993).

Fig 3. Our calculated high-pressure melting curve for Al (see Vočadlo and Alfè, 2002) is shown passing through a variety of recent high P experimental points.

Fig 4. Our calculated high P melting curve of Fe (plotted as a solid black line) is shown passing through the shock wave datum (open blue circle) of Brown and McQueen (1986). Other data shown includes: our melting curve corrected for the GGA pressure error (black dashed line), Belonoshko's melting curve (blue line), Belonoshko's melting data corrected for errors in potential fitting (black dots), Laio et al's melting curve (green line), Boehler's DAC curve (green dashed line), Shen's data (green diamonds), Yoo's shock data (open squares), William's melting curve (pale green dashed line).

Fig 5. Liquid and solid impurity mole fractions c_x^l and c_x^s of impurities X= S, Si and O, and resulting densities of the inner and outer core predicted by ab initio simulations. Solid, dashed and chain curves represent S, Si and O respectively. (a) liquid density ρ^l (kgm^{-3}); horizontal dotted line shows density from seismic data. (b) mole fractions in solid resulting from

equality of chemical potentials in solid and liquid. (c) relative density discontinuity ($\delta\rho/\rho^{l}$) at the ICB; horizontal dotted line is the value from free oscillation data.

Fig 6. Plot of bulk modulus (diamonds) and shear modulus (squares) for *hcp* Fe as a function of pressure, with values taken from Stixrude and Cohen (1995), Steinle-Neumann et al (1999), Söderlind et al (1996), Mao et al. (1999) and Vočadlo et al. (2003). Black diamonds and squares represent *ab initio* values, while white diamonds and squares represent values obtained from experimentally determined elastic constants.

Fig 7. Plot of aggregate v_P (diamonds) and v_S (squares) wave velocity for *hcp* Fe as a function of pressure, with values taken from Stixrude and Cohen (1995), Steinle-Neumann et al (1999), Söderlind et al (1996), Mao et al. (1999) and Vočadlo et al. (2003). Black diamonds and squares represent *ab initio* values, while white diamonds and squares represent values obtained from experimentally determined elastic constants. White circles are the experimental data of Fiquet et al. (2001).

Fig 8. The calculated stress tensors as a function of simulation time (upper row) and position correlation functions (lower row) for a 64 atom cubic supercell and temperature. The structure deviates away from the *bcc* phase below 3000K. We performed these high temperature calculations on two supercells to ensure that any transition observed is not influenced by the size and shape of the simulation cell. We used both the 64 atom cubic supercell and a hexagonal supercell (3x3x5) of 135 atoms, since this latter setting provides us with a simulation cell which readily allows us to have within it an integral number of unit cells of both the *bcc* and ω phases. The calculations were run initially at 6000K and then at

successively lower temperatures, using a stable equilibrated high temperature *bcc* configuration as the starting configuration in each case (Vočadlo et al., 2003).

Figure 1

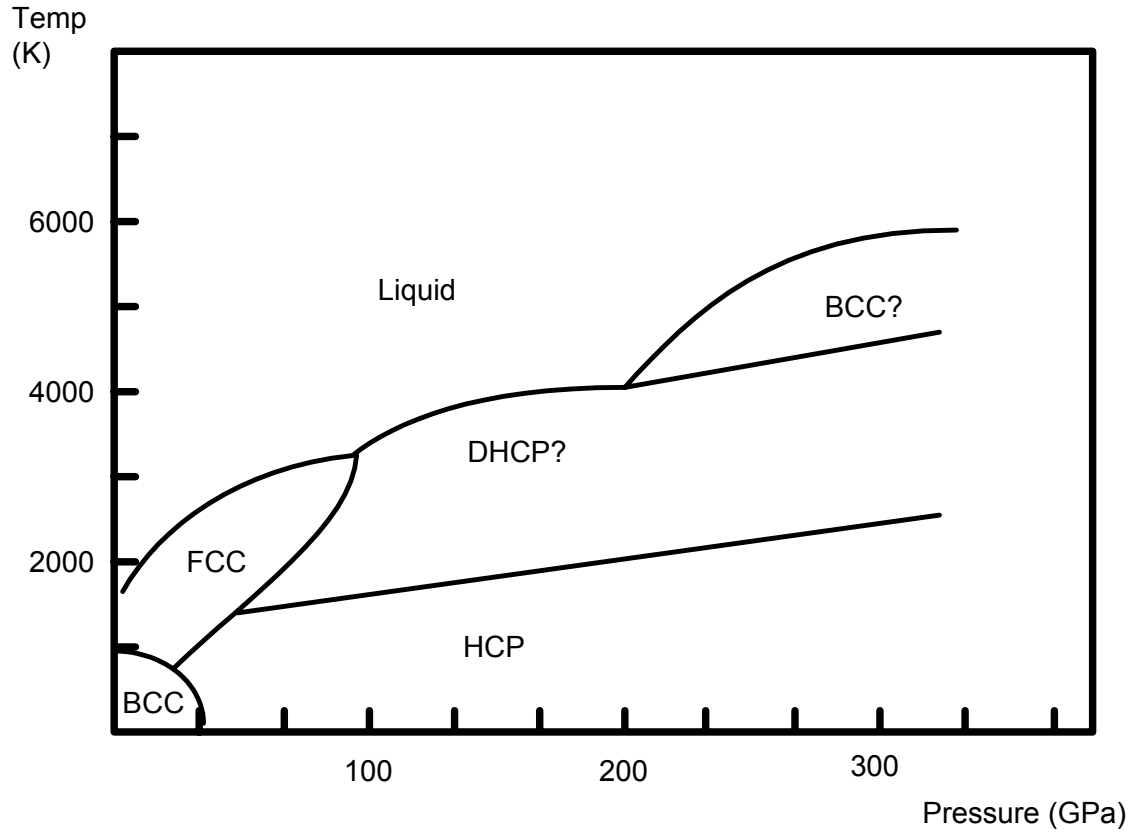
Temp
(K)
6000
4000
2000
Liquid
BCC?
DHCP?
FCC
HCP
BCC
100
200
300
Pressure (GPa)

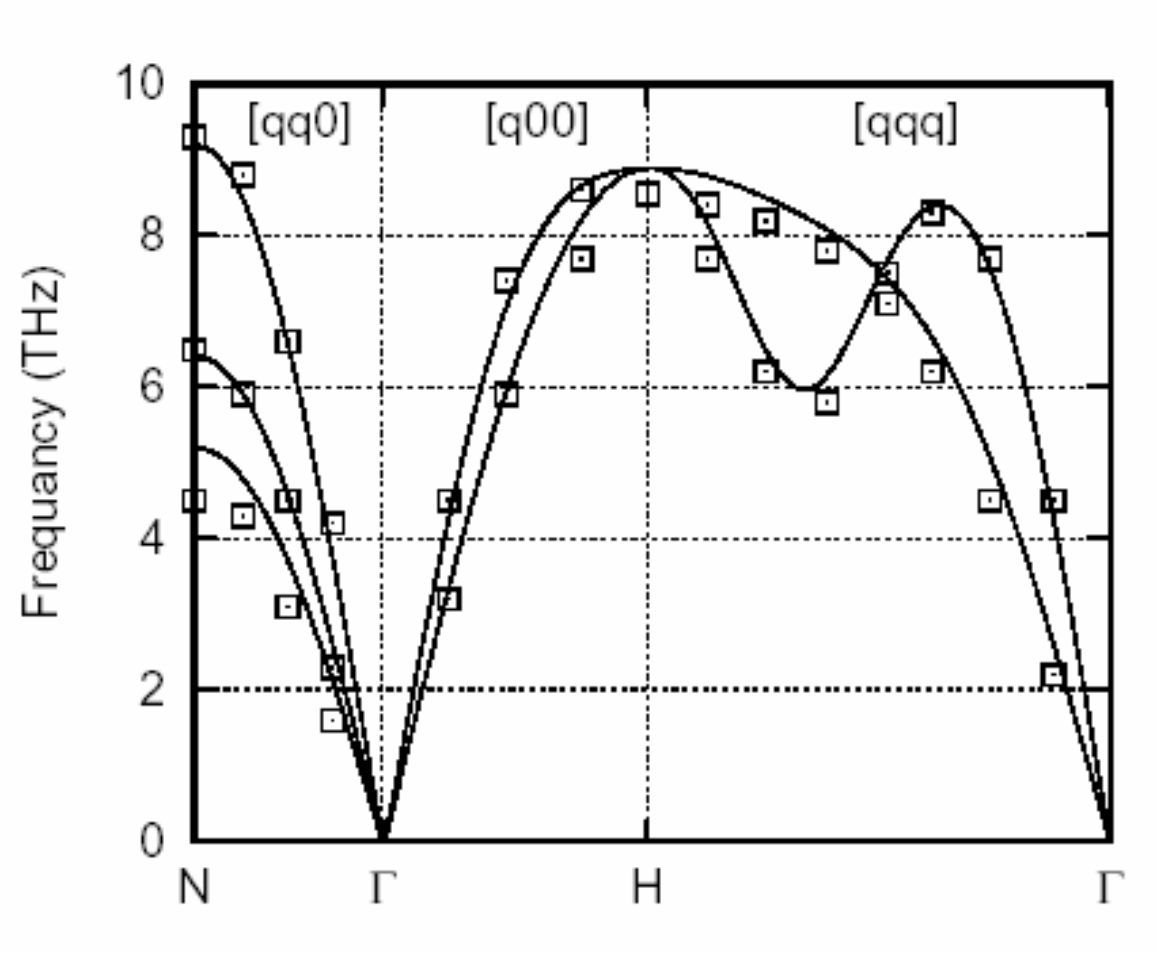
10
8
6
4
2
0
Frequancy (THz)
[qq0]
[q00]
[qqq]
N
Γ
H
Γ

Figure 3

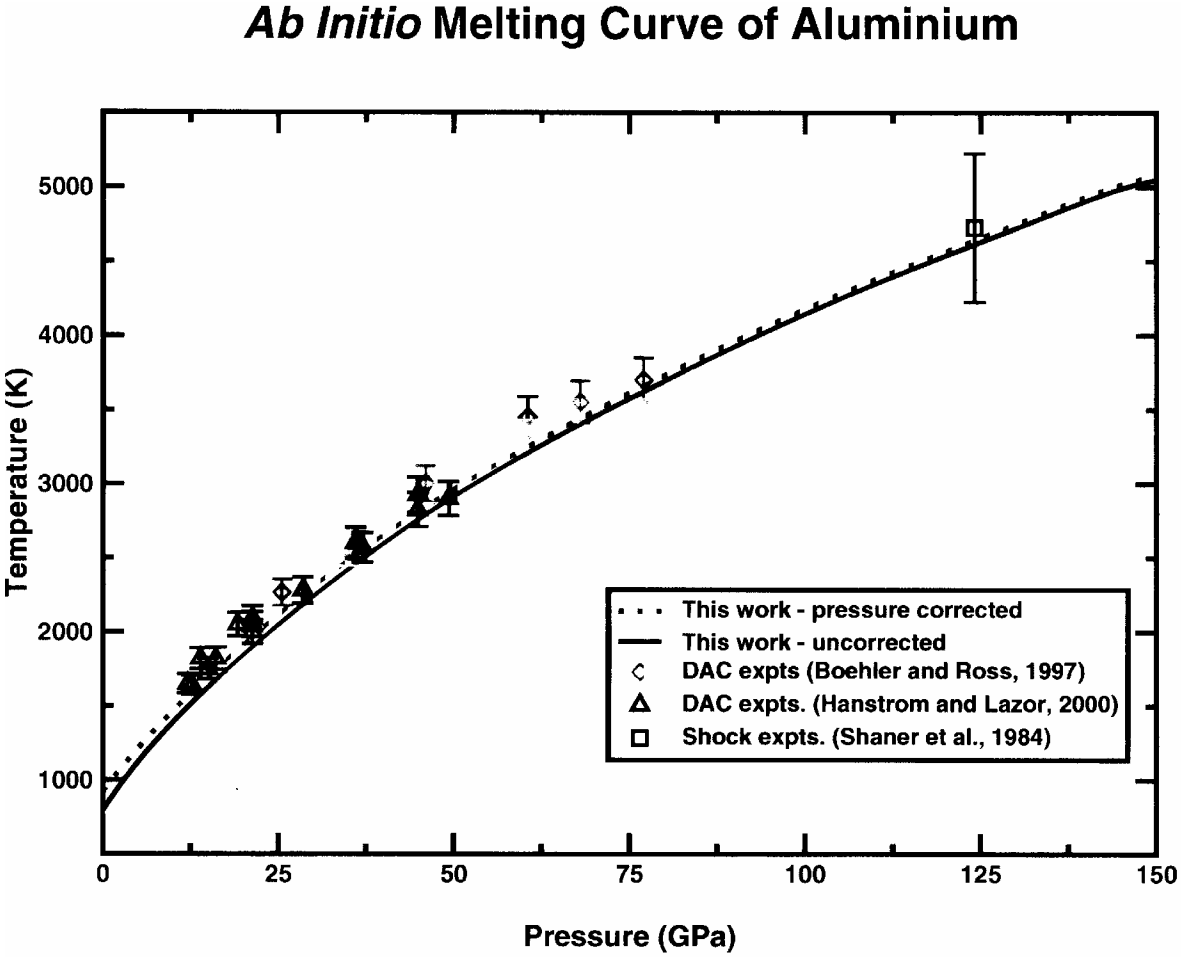
Ab Initio Melting Curve of Aluminium
Temperature (K)
5000
4000
3000
2000
1000
0
25
50
75
100
125
150
Pressure (GPa)
This work - pressure corrected
This work - uncorrected
DAC expts (Boehler and Ross, 1997)
DAC expts. (Hanstrom and Lazor, 2000)
Shock expts. (Shaner et al., 1984)

Figure 4

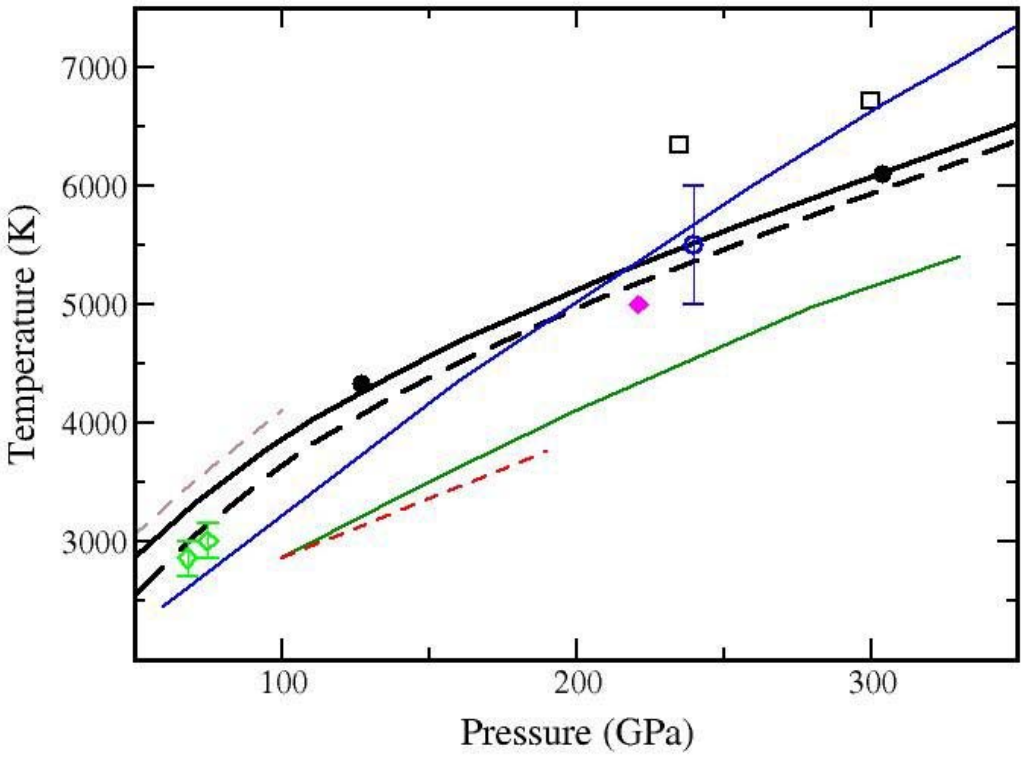
7000
6000
5000
4000
3000
Temperature (K)
100
200
300
Pressure (GPa)

Figure 5

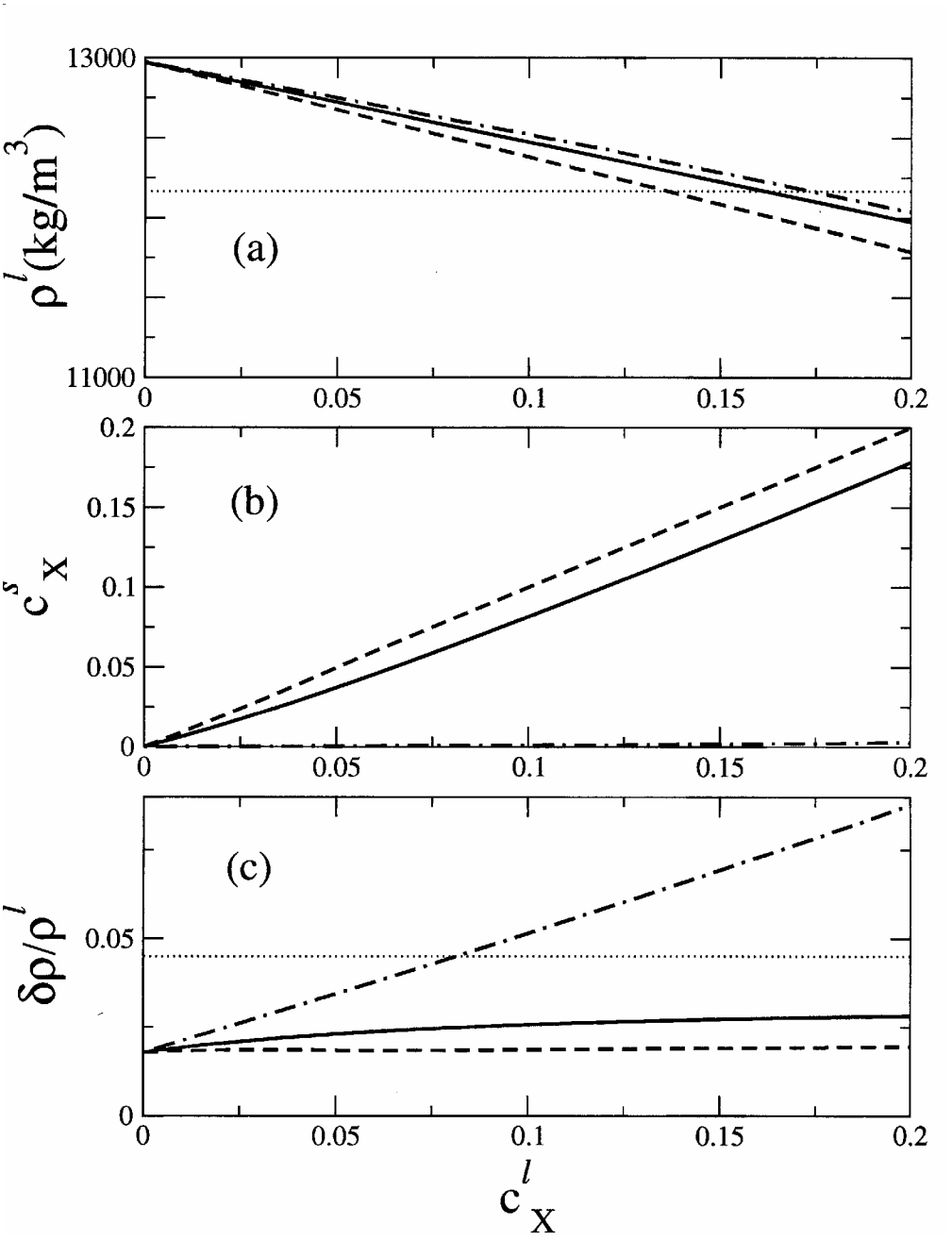
13000
11000
ρ^l(kg/m^3)
(a)
0
0.05
0.1
0.15
0.2
c^s_X
(b)
$\delta\rho/\rho^l$
(c)
c^l_X

Figure 6

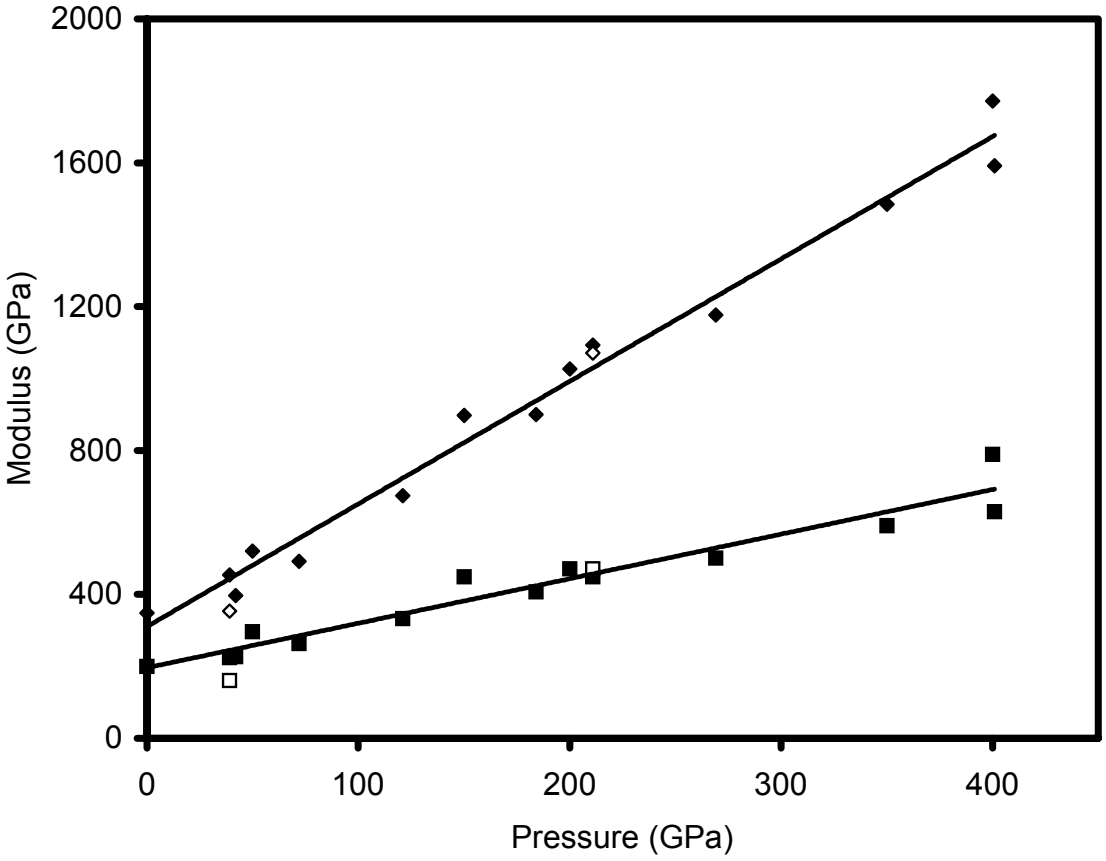
2000
1600
1200
800
400
0
Modulus (GPa)
0
100
200
300
400
Pressure (GPa)

Figure 7

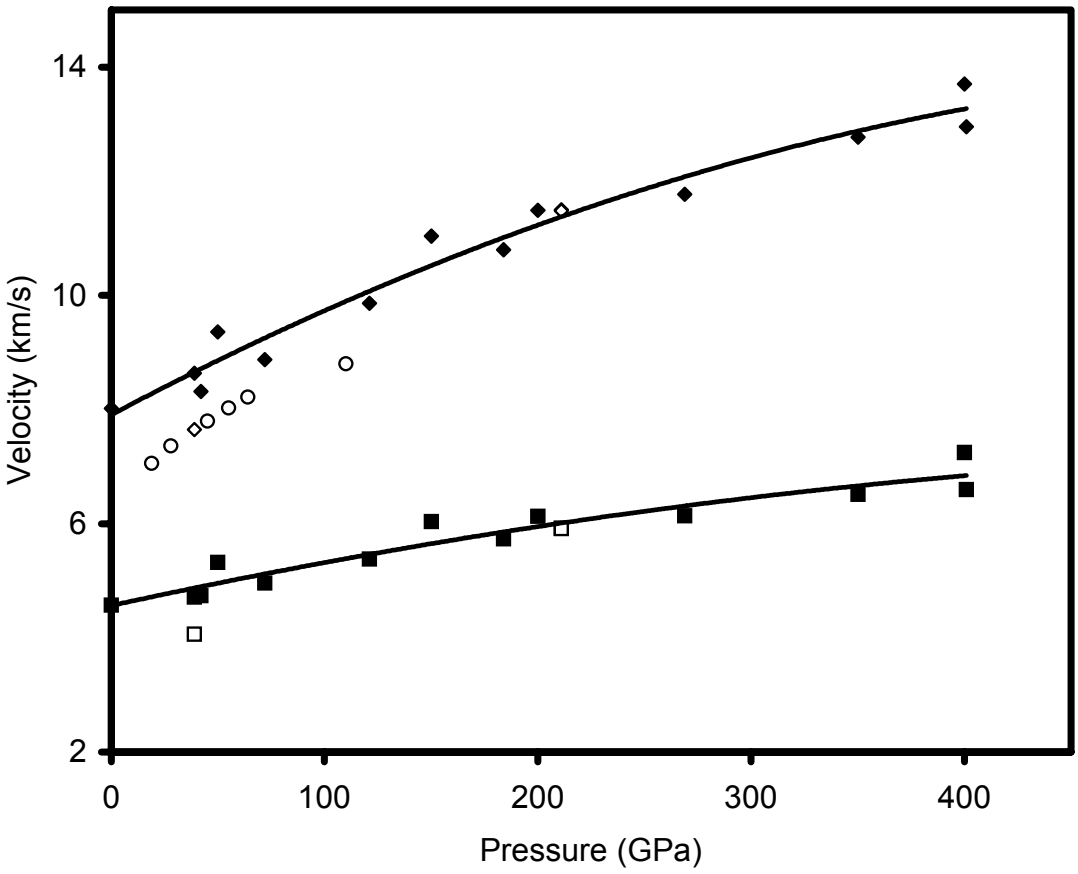

Figure 8.

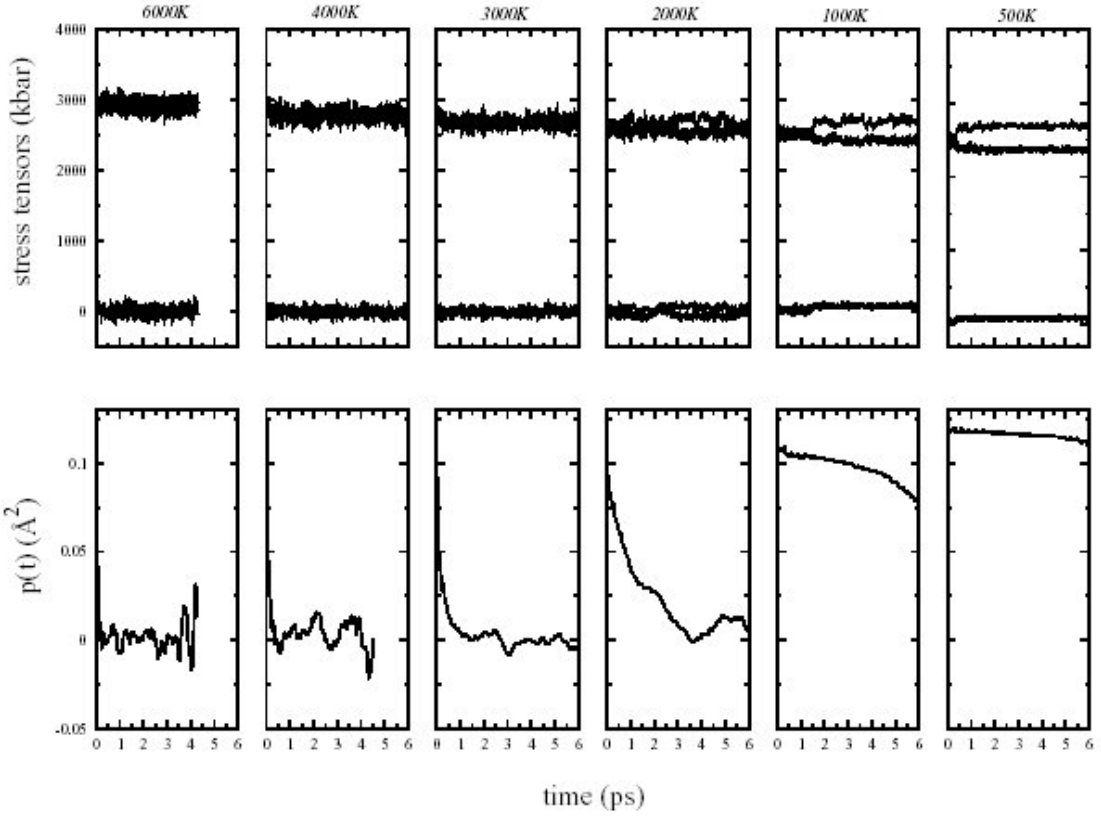
6000K
4000K
3000K
2000K
1000K
500K
stress tensors (kbar)
4000
3000
2000
1000
0
p(t) (Å^2)
0.1
0.05
0
-0.05
0 1 2 3 4 5 6
time (ps)